Fluctuation-dissipation theorem density-functional theory

Cite as: J. Chem. Phys. **122**, 164106 (2005); https://doi.org/10.1063/1.1884112
Submitted: 12 October 2004 . Accepted: 08 February 2005 . Published Online: 26 April 2005

Filipp Furche, and Troy Van Voorhis

Fluctuation-dissipation theorem density-functional theory

Filipp Furche
Institut für Physikalische Chemie, Universität Karlsruhe, Kaiserstraße 12, Karlsruhe 76128, Germany

Troy Van Voorhis[a)]
Department of Chemistry, Massachusetts Institute of Technology, Cambridge, Massachusetts 02139

(Received 12 October 2004; accepted 8 February 2005; published online 26 April 2005)

Using the fluctuation-dissipation theorem (FDT) in the context of density-functional theory (DFT), one can derive an exact expression for the ground-state correlation energy in terms of the frequency-dependent density response function. When combined with time-dependent density-functional theory, a new class of density functionals results that use approximations to the exchange-correlation kernel f^{xc} as input. This FDT-DFT scheme holds promise to solve two of the most distressing problems of conventional Kohn–Sham DFT: (i) It leads to correlation energy functionals compatible with exact exchange, and (ii) it naturally includes dispersion. The price is a moderately expensive $O(N^6)$ scaling of computational cost and a slower basis set convergence. These general features of FDT-DFT have all been recognized previously. In this paper, we present the first benchmark results for a set of molecules using FDT-DFT beyond the random-phase approximation (RPA)—that is, the first such results with $f^{xc} \neq 0$. We show that kernels derived from the adiabatic local-density approximation and other semilocal functionals suffer from an "ultraviolet catastrophe," producing a pair density that diverges at small interparticle distance. Nevertheless, dispersion interactions can be treated accurately if hybrid functionals are employed, as is demonstrated for He_2 and HeNe. We outline constraints that future approximations to f^{xc} should satisfy and discuss the prospects of FDT-DFT. © *2005 American Institute of Physics*. [DOI: 10.1063/1.1884112]

I. INTRODUCTION

Time-dependent density-functional theory (TDDFT)[1,2] has developed into an accurate and inexpensive tool for describing excited state properties, energies and response properties of a variety of systems (see, e.g., Refs. 3–5). It is somewhat less widely appreciated that TDDFT also provides an alternative prediction of static *ground-state* properties via the fluctuation-dissipation theorem (FDT). The FDT was first derived by Callen and Welton in 1951, who used it to relate the mean square fluctuation of a local one-particle observable in the ground state Ψ_0 to the imaginary (dissipative) part of the density-density response function $\chi(x_1,x_2;\omega)$,

$$\langle\Psi_0|(O-\langle O\rangle)^2|\Psi_0\rangle = -\operatorname{Im}\int_0^\infty \frac{d\omega}{\pi}\int dx O(x)\chi(x,x;\omega)O(x); \tag{1}$$

as usual, $x=(\mathbf{r},\sigma)$ denotes a set of space-spin coordinates. The FDT may be considered as a special sum rule. The frequency integral over the imaginary part of χ is used to generate a resolution of the identity, as is easy to verify by inserting the Lehmann representation of χ (Ref. 6) into Eq. (1),

$$\chi(x_1,x_2;\omega) = -\sum_{n\neq 0}\left(\frac{\langle\Psi_0|\hat\rho(x_1)|\Psi_n\rangle\langle\Psi_n|\hat\rho(x_2)|\Psi_0\rangle}{\Omega_n-\omega-i\eta} + \frac{\langle\Psi_0|\hat\rho(x_2)|\Psi_n\rangle\langle\Psi_n|\hat\rho(x_1)|\Psi_0\rangle}{\Omega_n+\omega+i\eta}\right). \tag{2}$$

In the last equation, $\hat\rho(x)$ denotes the density operator, the Ψ_n are excited states with excitation energies Ω_n, and $\eta\to 0$ is used to indicate that χ is analytic in the upper half of the complex ω plane.

An intriguing aspect of the FDT is that it can be used to factorize *two-particle* quantities into a sum over *one-particle* quantities. In the constrained-search formulation of density-functional theory[7] we consider an N electron system with a scaled Coulomb interaction α/r_{12}, whose ground-state density $\rho_\alpha(x)$ is fixed at the physical value $\rho(x)\equiv\rho_\alpha(x)|_{\alpha=1}$; thus $\alpha=0$ corresponds to the noninteracting Kohn–Sham (KS) system.[8] Langreth and Perdew generalized the FDT[9,10] to obtain an expression for the correlated part of the pair density,

$$P^c_\alpha(x_1,x_2) = -\operatorname{Im}\int_0^\infty \frac{d\omega}{\pi}(\chi_\alpha(x_1,x_2;\omega)-\chi_0(x_1,x_2;\omega)). \tag{3}$$

The correlation energy is obtained from P^c_α via coupling-strength integration,

[a)]Electronic mail: tvan@mit.edu

$$E^c = \frac{1}{2}\int_0^1 d\alpha \int dx_1 dx_2 \frac{P_\alpha^c(x_1,x_2)}{r_{12}}. \quad (4)$$

On the other hand, χ_α describes the response of the one-particle density, and is therefore accessible from time-dependent density-functional response theory.[11] More precisely, for a pure density functional χ_α satisfies the Dyson-type equation[12–14]

$$\chi_\alpha(x,x';\omega) = \chi_0(x,x';\omega) + \int dx_1 dx_2 \chi_0(x,x_1;\omega) \times\left(\frac{1}{r_{12}} + f_\alpha^{\mathrm{xc}}(x_1,x_2;\omega)\right)\chi_\alpha(x_2,x';\omega). \quad (5)$$

We stress again that this is an *exact* expression for the correlation energy that has been known for quite some time. In practice, one can compute all excitation energies and transition densities to construct χ_α from its Lehmann representation. Thus, for a given *approximate* exchange-correlation (XC) functional, where f^{xc} and χ_0 are both given as explicit functionals of the density, Eqs. (3)–(5) define the FDT-DFT correlation energy as a functional of ρ.

Conventional DFT directly uses parametrizations of the XC energy functional $E^{\mathrm{xc}}[\rho]$, as obtained, e.g., within the local-density approximation (LDA) or the generalized gradient approximation (GGA). At first sight, the FDT-DFT scheme appears to be an unnecessary detour, especially since computing the full response function χ_α from Eq. (5) is computationally much more demanding than a conventional DFT calculation. However, FDT-DFT still produces useful results even in the simplest possible approximation, $f^{\mathrm{xc}}=0$, which corresponds to the random-phase approximation (RPA);[9,10,15,16] this is certainly not true for the Hartree approximation ($E^{\mathrm{xc}}[\rho]=0$) of conventional DFT. Moreover, RPA correlation energies are compatible with exact exchange and include some dispersion, which is very difficult to achieve with semilocal functionals. For dynamical correlation, one hopes that FDT-DFT approximations can approach the accuracy of coupled cluster methods such as coupled cluster with single and double and perturbative triple excitations [CCSD(T)].[17] Moreover, because FDT-DFT is based on a density-functional reference, it holds promise for metal clusters and other small gap systems where Hartree–Fock (HF)-based single reference methods often fail.[18,19] For nearly uniform systems, this goal has actually been achieved.[20] Another advantage of FDT-DFT is the link between ground-state theory and TDDFT; apart from the ground-state density (or, equivalently, the independent particle Hamiltonian that generates this density), both approaches depend on the XC kernel as input only. Ideally, both fields will benefit from progress in approximations to f^{xc}.

FDT-DFT beyond the RPA has been applied only to a few cases—the uniform electron gas,[21,22] jellium models,[23–25] and a selection of few electron systems.[25,26] For the uniform gas, accurate parametrizations of f^{xc} are available[27] that yield virtually exact results for the correlation energy per particle in the FDT-DFT scheme,[21] but much less is known about f^{xc} in nonuniform systems. In the present work, we extend the basis set approach to FDT-DFT beyond the RPA and present applications of the formalism to nonuniform systems. Through several numerical applications, we showcase the appealing features of FDT-DFT (e.g., the natural treatment of dispersion). However, we also demonstrate that standard semilocal (GGA and hybrid) approaches predict a *divergent* electron-electron cusp condition. This rather serious limitation argues strongly for the development of nonlocal approximations to f^{xc}.

II. THEORY

A. FDT-DFT formalism

To evaluate Eqs. (3)–(5) we use an extension of the formalism developed previously by one of us.[11,15] Here, we only reiterate the crucial points.

All our calculations will be performed in a finite basis of one-particle orbitals. In this case, the TDDFT response is naturally expressed in the Hilbert space $L_{\mathrm{occ}}\otimes L_{\mathrm{virt}}\oplus L_{\mathrm{virt}}\otimes L_{\mathrm{occ}}$, where $L_{\mathrm{occ}}(L_{\mathrm{virt}})$ is the space of occupied (virtual) Kohn–Sham orbitals, denoted by indices $i,j,k\ldots(a,b,c\ldots)$. We will generalize the previous treatment to allow for hybrid functionals, containing an admixture $\gamma\geqslant 0$ of exact exchange.[28] The key quantities are the so-called orbital rotation Hessians $(A_\alpha \pm B_\alpha)$,

$$(A_\alpha - B_\alpha)_{iajb} \equiv (\epsilon_a - \epsilon_i)\delta_{ij}\delta_{ab} + \gamma\alpha(\langle ij|ba\rangle - \langle ia|jb\rangle),$$

$$(A_\alpha + B_\alpha)_{iajb} \equiv (\epsilon_a - \epsilon_i)\delta_{ij}\delta_{ab} - \gamma\alpha(\langle ij|ba\rangle + \langle ia|jb\rangle) + 2\langle ij|ab\rangle + 2f_{\alpha iajb}^{\mathrm{xc}}.$$

$\langle ij|ab\rangle$ denotes a two-electron repulsion integral (in Dirac notation); the $\phi_p(x)$ are the ground-state KS orbitals with orbital energies ϵ_p.

$$f_{\alpha iajb}^{\mathrm{xc}} \equiv \int dx_1 dx_2 \phi_i(x_1)\phi_a(x_1) f_\alpha^{\mathrm{xc}}(x_1,x_2)\phi_j(x_2)\phi_b(x_2) \quad (6)$$

is a matrix representation of the XC kernel at coupling strength α, $f_\alpha^{\mathrm{xc}}(x_1,x_2)$, which is a functional of the ground-state density. In the adiabatic approximation (AA), the frequency dependence of f_α^{xc} is neglected by taking the static limit,[2,29]

$$f_\alpha^{\mathrm{xc}}(x_1,x_2) \equiv \frac{\delta^2 E_\alpha^{\mathrm{xc}}}{\delta\rho(x_1)\delta\rho(x_2)}. \quad (7)$$

$E_\alpha^{\mathrm{xc}}[\rho]$ is related to the XC energy functional at full coupling strength $E^{\mathrm{xc}}[\rho]\equiv E_\alpha^{\mathrm{xc}}[\rho]|_{\alpha=1}$ (*without* the admixture of exact exchange) via the relation[30]

$$E_\alpha^{\mathrm{xc}}[\rho] = \alpha^2 E^{\mathrm{xc}}[\rho_{1/\alpha}], \quad (8)$$

where $\rho_\lambda(\mathbf{r},\sigma)=\lambda^3\rho(\lambda\mathbf{r},\sigma)$ is a scaled density, with uniform scaling parameter λ. An analogous identity for the frequency-dependent XC kernel can be derived[21] from the scaling behavior of the time-dependent XC potential.[31]

The RPA is recovered in the limiting case $f_\alpha^{\mathrm{xc}}(x_1,x_2)=0$. The bare RPA in a density-functional context corresponds to $\gamma=0$, while the HF-based RPA with exchange results corresponds to $\gamma=1$, provided that HF orbitals and orbital ener-

gies are used. From this perspective, f_α^{xc} gives rise to a static local-field correction[32] that accounts for effects beyond the RPA.

The coupling-strength integrand can be constructed directly in terms of the response matrices if we introduce the correlation part of the two-particle density matrix P_α^c,

$$P_\alpha^c = (A_\alpha - B_\alpha)^{1/2} M_\alpha^{-1/2} (A_\alpha - B_\alpha)^{1/2} - \mathbf{1}, \tag{9}$$

where

$$M_\alpha = (A_\alpha - B_\alpha)^{1/2} (A_\alpha + B_\alpha)(A_\alpha - B_\alpha)^{1/2}. \tag{10}$$

Then Eq. (4) becomes

$$E^{c\ \mathrm{FDT\text{-}DFT}} = \frac{1}{2}\int_0^1 d\alpha \sum_{iajb} \langle ij|ab\rangle P^c_{\alpha iajb}. \tag{11}$$

The FDT-DFT XC energy is obtained by adding this correlation energy to the exact exchange energy,

$$E^{\mathrm{xc\ FDT\text{-}DFT}} = -\frac{1}{2}\sum_{ij}\langle ij|ji\rangle + \frac{1}{2}\int_0^1 d\alpha \sum_{iajb}\langle ij|ab\rangle P^c_{\alpha iajb}. \tag{12}$$

Because the ground-state KS orbitals are uniquely fixed by the density, $E^{\mathrm{xc\ FDT\text{-}DFT}}$ is a functional of the density as well.

B. Stability

The FDT-DFT formalism is based on the tacit assumption that the response calculated from an approximate XC kernel is qualitatively similar to the exact response. Most notably, we require that none of the approximate excitation energies are *imaginary*, or else the use of the Lehmann representation [Eq. (2)] is questionable. As first shown by Bauernschmitt and Ahlrichs,[33] an approximate functional gives real excitation energies only if the matrices $(A_\alpha \pm B_\alpha)$ are positive semidefinite. These *stability conditions* hold for any value of the coupling constant and are hence a powerful constraint on approximations to f^{xc}. In our FDT-DFT approach, instabilities are easily detected because they lead to negative eigenvalues of the matrix M_α defined in Eq. (10) and, consequently, to *imaginary correlation energies*!

What is the physical origin of imaginary excitation energies? The exact χ_α has poles at real, non-negative excitation energies for all α because it describes the response of a ground state for all α by construction. An approximate χ_α, generated from an approximate XC kernel, may violate this condition in one of two ways: (1) The KS ground state may be connected to an *excited state* at finite α due to the influence of strong multireference correlation in the system (e.g., singlet-triplet instabilities in the response matrix). (2) The response can be artificially spoiled by a mismatch between the definition of f^{xc} and the orbitals (or equivalently, the potential) used to define χ_0. For example, say one has a system where van Leeuwen–Baerends 1994 (LB94)[34] predicts a singlet ground state for some value of α, while LDA predicts a triplet ground state for this same value of α. Then, if we use LB94 to approximate χ_0 (i.e., we use the LB94 orbitals and eigenvalues) and then compute the response using $f^{\mathrm{xc}}_{\mathrm{LDA}}$, the response will have an imaginary eigenvalue due to the fact that the LB94 reference is *not* the ground state at this intermediate value of α.

We will term these two effects *physical* and *artifactual* instabilities, respectively. Our desire to avoid artifactual instabilities leads us to focus our attention on *consistent* choices of χ_0 and f^{xc}. That is, we consider χ_0 and f^{xc} to be derived from a single exchange-correlation energy functional. For the semilocal functionals used in this paper, we have found only two cases (Cl atom and NO molecule within the local spin-density approximation) where this leads to an instability. On the other hand, if χ_0 and f^{xc} are chosen inconsistently, we find in practice that instabilities are encountered ca. 10% of the time. This should not be confused with a *self-consistent* treatment of the FDT-DFT energy functional[35] which is beyond our present scope.

III. SHORT-RANGE BEHAVIOR OF THE PAIR DISTRIBUTION FUNCTION

Local-field corrections have a long history in the theory of uniform systems (see, e.g., Ref. 36 for a recent overview). Their original motivation was to remedy the spurious behavior of the RPA pair density at small inter-electron separations. Most work in uniform gas theory focuses on the pair distribution function (PDF), g_α, that gives the conditional probability of finding an electron at $\mathbf{r}'$ given that another electron is located at $\mathbf{r}$; its correlated part is closely related to the correlated part of the pair density,

$$g_\alpha^c(\mathbf{r}_1,\mathbf{r}_2) \equiv \frac{\Sigma_{\sigma_1\sigma_2} P_\alpha^c(x_1,x_2)}{\rho(\mathbf{r}_1)\rho(\mathbf{r}_2)}. \tag{13}$$

In the last equation, $\rho(\mathbf{r}) = \Sigma_\sigma \rho(x)$ is the total density. The uniform gas PDF is known accurately.[37] In the present formalism, $P_\alpha^c(x_1,x_2)$ is obtained from the correlated part of the two-particle density matrix defined in Eq. (9),

$$P_\alpha^c(x_1,x_2) = \sum_{iajb} P^c_{\alpha iajb}\phi_i(x_1)\phi_a(x_1)\phi_j(x_2)\phi_b(x_2). \tag{14}$$

The exact PDF is finite at $r_{12}=0$ and satisfies a cusp condition.[38,39] How does a semilocal XC kernel affect the short-range behavior of g_α? The adiabatic local spin-density approximation (ALDA) energy expression

$$E_\alpha^{\mathrm{xc\ ALDA}}[\rho] = \alpha^5 \int d^3r F(\alpha^{-3}\rho(x)) \tag{15}$$

implies that the XC kernel

$$f_\alpha^{\mathrm{xc\ ALDA}}(x_1,x_2) = \frac{1}{\alpha}\frac{\partial^2 F(\alpha^{-3}\rho(x_1))}{\partial\rho(\mathbf{r}_1,\sigma_1)\partial\rho(\mathbf{r}_1,\sigma_2)}\delta(\mathbf{r}_1-\mathbf{r}_2) \tag{16}$$

is proportional to a three-dimensional delta function. We restrict ourselves to the ALDA in the following (rather qualitative) discussion; gradient corrections lead to additional terms that behave like derivatives of $\delta(\mathbf{r}_1-\mathbf{r}_2)$.

A. Uniform systems

It is well known that the ALDA kernel [Eq. (16)] is incorrect even for uniform systems (see, e.g., Ref. 40 for a review of properties of the uniform gas XC kernel). In the

uniform gas, g^c_α, χ_α, and f^{xc}_α depend only on the inter-electron distance r_{12}. We consider the spin-unpolarized case here. g^c_α can be obtained from the correlation part of the static structure factor at coupling strength α, $S^c_\alpha(q)$, by Fourier transformation,

$$g^c_\alpha(r_{12}) = \frac{9\pi^2}{2k_F^6 r_{12}} \int_0^\infty dq q \sin(qr_{12}) S^c_\alpha(q). \tag{17}$$

In the last equation, $k_F=(3\pi^2\rho)^{1/3}$ denotes the Fermi wave vector. $S^c_\alpha(q)$ itself is related to the XC kernel via

$$S^c_\alpha(q) = -\,\mathrm{Im} \int_0^\infty \frac{d\omega}{\pi} \overline{\chi}_0(q;\omega) \left(\alpha \frac{4\pi}{q^2} + \overline{f}^{\mathrm{xc}}_\alpha(q) \right) \overline{\chi}_\alpha(q;\omega), \tag{18}$$

where Fourier-transformed quantities are denoted by a bar, e.g.,

$$\overline{f}^{\mathrm{xc}}_\alpha(q) = \frac{4\pi}{q} \int_0^\infty dr_{12} r_{12} \sin(qr_{12}) f^{\mathrm{xc}}_\alpha(r_{12}). \tag{19}$$

Equations (17) and (18) are equivalent to the definition of the pair density within FDT-DFT given in Eq. (3), but apply to spin-unpolarized uniform systems only.

According to Eq. (17), small r_{12} behavior of $g^c_\alpha(r_{12})$ is determined by the large-q behavior of $S^c_\alpha(q)$. We consider only the case of small coupling strength α here. The lowest-order contribution to $S^c_\alpha(q)$ is obtained by setting $\overline{\chi}_\alpha(q;\omega) = \overline{\chi}_0(q;\omega)$ in Eq. (18). For large q, the frequency integration can be carried out,[41]

$$S^c_\alpha(q) = -\,\alpha \frac{4k_E^5}{9\pi^4 q^2} \left(\frac{4\pi}{q^2} + \overline{f}^{x}(q) \right), \quad q \to \infty, \quad \alpha \to 0. \tag{20}$$

As noted by Kimball,[41] $S^c_\alpha(q)$ should decay as $1/q^4$ for large q to make the PDF finite at the origin. This implies that $\overline{f}^x(q) \propto 1/q^2$ for $q \to \infty$, i.e., the exchange kernel used in FDT-DFT within the AA should not diverge faster than $1/r_{12}$ at small r_{12}. On the other hand, $\overline{f}^{\mathrm{ALDA}}(q)$ is a constant, which leads to

$$g^{c\ \mathrm{ALDA}}(r_{12}) \propto \frac{1}{r_{12}}, \quad r_{12} \to 0, \tag{21}$$

i.e., the short-ranged ALDA kernel makes $g^{c\ \mathrm{ALDA}}$ diverge at small interparticle distances, at least in the limit of small α. This "ultraviolet catastrophe" of the ALDA may be related to the fact that

$$\overline{f}^{x\ \mathrm{ALDA}} = \lim_{q\to 0} \overline{f}^x(q), \tag{22}$$

i.e., the ALDA kernel corresponds to the *small q* limit of the exact static exchange kernel. The literature is largely silent on this pathological aspect of the ALDA, except for a hint in the work of Dobson and Wang[24] who mention in passing a weak divergence of the PDF at small r_{12}, but do not give further details.

B. Small coupling strength (high-density) limit

For small coupling strength α, a perturbation expansion for P^c_α may be derived from Eq. (9),

$$P^c_{\alpha iajb} = -\,2\alpha \frac{\langle ij|ab\rangle + f^x_{iajb}}{\epsilon_a + \epsilon_b - \epsilon_i - \epsilon_j}, \tag{23}$$

where f^x is defined via

$$f^x(x_1,x_2) = \lim_{\alpha\to 0} \frac{1}{\alpha} f^{\mathrm{xc}}_\alpha(x_1,x_2). \tag{24}$$

To extract the short-range behavior of P^c_α at small α, we expand it into pair contributions,

$$P^c_\alpha(x_1,x_2) = 2\alpha \sum_{ij} \psi^{(0)}_{ij}(x_1,x_2) \psi^{(1)}_{ij}(x_1,x_2) + O(\alpha^2), \tag{25}$$

where $\psi^{(0)}_{ij}(x_1,x_2) = \phi_i(x_1)\phi_j(x_2)$. To recover Eq. (23), the first-order geminals $\psi^{(1)}_{ij}$ must satisfy

$$\begin{aligned}(H(x_1) + H(x_2) - (\epsilon_i + \epsilon_j))\psi^{(1)}_{ij}(x_1,x_2) \\ = -\,(U^{(1)}(x_1,x_2) - E^{(0)}_{ij})\psi^{(0)}_{ij}(x_1,x_2),\end{aligned} \tag{26}$$

subject to the orthonormality constraint $\langle \psi^{(1)}_{ij} | \psi^{(0)}_{kl} \rangle = 0$ for all i,j,k,l. Here, H is the effective one-particle Hamiltonian of the KS ground state,

$$U^{(1)}(x_1,x_2) = \frac{1}{r_{12}} + f^x(x_1,x_2), \tag{27}$$

is a first-order effective interaction, and $E^{(0)}_{ij} = \langle \psi^{(0)}_{ij} | U^{(1)} | \psi^{(0)}_{ij} \rangle$. We now turn to the ALDA. Since Eq. (26) is linear, we may decompose the first-order geminal into an RPA part and a singular part

$$\psi^{(1)\mathrm{ALDA}}_{ij}(x_1,x_2) = \psi^{(1)\mathrm{RPA}}_{ij}(x_1,x_2) + \psi^{(1)\mathrm{sing}}_{ij}(x_1,x_2). \tag{28}$$

$\psi^{(1)\mathrm{RPA}}_{ij}$ is the solution of Eq. (26) within the RPA, i.e., $f^x(x_1,x_2)=0$. $\psi^{(1)\mathrm{RPA}}_{ij}$ is well behaved at the origin and satisfies the first-order cusp condition. The singular part must satisfy

$$\begin{aligned}(H(x_1) + H(x_2) - (\epsilon_i + \epsilon_j))\psi^{(1)\mathrm{sing}}_{ij}(x_1,x_2) \\ = (f^x(x_1,x_2) - E^{(0)}_{ij})\psi^{(0)}_{ij}(x_1,x_2) \\ \times\!\propto \delta(\mathbf{r}_1 - \mathbf{r}_2)\delta_{\sigma_1\sigma_2}\psi^{(0)}_{ij}(x_1,x_2), \quad r_{12}\to 0.\end{aligned} \tag{29}$$

The singularity on the right-hand side can be canceled only if $\psi^{(1)\mathrm{sing}}_{ij}$ behaves as

$$\psi^{(1)\mathrm{sing}}_{ij}(x_1,x_2) \propto \frac{1}{r_{12}} \delta_{\sigma_1\sigma_2}, \quad r_{12}\to 0. \tag{30}$$

This implies that $P^{c\ \mathrm{ALDA}}_\alpha$ and $g^{c\ \mathrm{ALDA}}_\alpha$ exhibit a $1/r_{12}$ divergence to first order in α, which generalizes the result of the last section.

C. General case

It is very difficult to address the precise short-range behavior of the FDT-DFT pair density function for finite values of the coupling constant α. This is mainly because $P^c_\alpha(x_1,x_2)$ is not directly related to a wave function in the present approach. It seems likely that the behavior observed in first

order in α is not remedied at stronger coupling. One even has to face the possibility that P_α^c behaves worse for finite α. Caution seems appropriate in view of the pathological discontinuities of the wave function at small interparticle separation observed for three-dimensional attractive delta interactions at any finite coupling strength.[42]

Given that P_α^c can diverge at the origin in certain circumstances, one begins to wonder if the correlation energy predicted by ALDA-FDT-DFT can also be infinite. The first-order term proportional to $1/r_{12}$ gives a *finite* contribution to the second-order correlation energy. We cannot, however, rule out the possibility that higher-order contributions to the correlation energy are divergent. On the other hand, in the case of GGA functionals, a similar analysis at weak coupling uncovers an apparent $1/r_{12}^2$ divergence in the PDF, which, taken by itself, would lead to a divergent correlation energy. In this situation, the challenge arises in how different divergent quantities can be added to (and subtracted from) one another as different terms in the coupling strength and gradient expansions are summed up. It is therefore not clear if one should expect a finite correlation energy from semilocal FDT-DFT.

D. Basis set approach

In a finite basis, the divergence of g_α can only be described *approximately*, and thus the finite basis estimates of E_c will always be finite. In what follows, then, we turn our attention to the obvious question: Can reasonable approximations to E_c be found by applying FDT-DFT within a large but finite basis? In this respect, it is important to note that the expected divergence of P_α^c will result in a *very* slow convergence of the correlation energy with basis set size. For example, if we assume that the pair density behaves as $1/r_{12}$ at short distances, then standard techniques[43,44] show that the lth partial-wave contribution to E_c scales asymptotically as

$$E_c(l) \propto \frac{1}{(l+1)(l+2)}, \tag{31}$$

which means that in a basis that is composed of a complete set of functions up to a maximum angular momentum $l_{\max}$, the correlation energy will scale as

$$E_c \propto \sum_{l=0}^{L_{\max}} \frac{1}{(l+1)(l+2)} = \frac{l_{\max}}{l_{\max}+1/2} \tag{32}$$

for large $l_{\max}$. This convergence is much slower than the conventional case,

$$E_c^{\mathrm{conv}} \propto \frac{1}{(l_{\max}+1/2)^3}. \tag{33}$$

On the other hand, we can test the predicted short-range behavior of the PDF by comparing Eq. (32) to results of calculations in large basis sets.

IV. IMPLEMENTATION AND COMPUTATIONAL DETAILS

Our FDT-DFT code is based on the RPA implementation described in Ref. 15, which is part of TURBOMOLE.[45,46] Each calculation involves threes steps: (1) A ground-state DFT calculation produces the orbitals and eigenvalues. (2) Using these orbital and eigenvalues as input, a TDDFT response calculation is performed (using the f^{xc} appropriate to the ground-state functional) to construct the FDT-DFT correlation energy [Eqs. (11)]. (3) This correlation energy is combined with the exact exchange energy computed using the same orbitals to obtain the exchange-correlation energy [Eq. (12)]. For large systems, the rate-determining step is the computation of the square root of M [and $(A-B)$ for hybrid functionals], which scales as N^6 if N measures the system size. This is the same for all semilocal XC kernels within the AA. Our algorithm gives the exact coupling-strength integrand within the RPA, and a nearly exact one if f^{xc} is evaluated on a numerical grid.

The only modification of the RPA algorithm necessary for FDT-DFT concerns the definition of $(A_\alpha+B_\alpha)$. For each coupling-strength integration point, the integrals $f_{\alpha iajb}^{\mathrm{xc}}$ have to be added to the RPA part of $(A_\alpha+B_\alpha)$. Within the adiabatic GGA

$$E_\alpha^{\mathrm{xc\ AGGA}}[\rho] = \alpha^5 \int d^3r F(\alpha^{-3}\rho(x), \alpha^{-4}\nabla\rho(x)). \tag{34}$$

Defining a first-order density

$$\rho^{(1)}(x) = \rho(x) + \sum_{ia} U_{ia}\phi_i(x)\phi_a(x), \tag{35}$$

analytical expressions for the matrix elements of f_α^{xc} are conveniently derived from

$$f_{\alpha iajb}^{\mathrm{xc}} = \left.\frac{\partial E_\alpha^{\mathrm{xc}}[\rho^{(1)}]}{\partial U_{ia}\partial U_{jb}}\right|_{U=0.} \tag{36}$$

The quadrature over $\mathbf{r}$ is done numerically using standard molecular integration schemes.[47] Since there are $O(N^4)$ integrals $f_{\alpha iajb}^{\mathrm{xc}}$, this is an N^5 step. The transformation to compute the integrals $\langle ij|ab\rangle$ has the same scaling; however, except in the exchange-only case the $f_{\alpha iajb}^{\mathrm{xc}}$ have to be constructed for each α integration point, because $f_{\alpha iajb}^{\mathrm{xc}}$ is nonlinear in α. The evaluation of the orbital products $\phi_i(x)\phi_a(x)$ on the molecular grid is an N^3 step that is done before the coupling-strength integration starts. Our code takes advantage of non-Abelian point-group symmetry. This is achieved by the reduction of $L_{\mathrm{occ}}\otimes L_{\mathrm{virt}}$ into irreducible tensor spaces, on the one hand, and the use of integration points that are nonredundant by symmetry, on the other. Thus, the total cost for computing $f_{\alpha iajb}^{\mathrm{xc}}$ is reduced approximately by a factor of g^2, where g is the order of the point group. For the small, highly symmetric systems considered in this work, g^2 is typically around 100 or larger.

The ground-state energies and orbitals were generated with the DSCF module of TURBOMOLE. Tight convergence of the density matrix (10^{-7} a.u.), fine integration grids (size 5, Ref. 47) and accurate coupling-constant integration (7 points) were used throughout. A further increase in the size of either grid did not change the results significantly, as was verified in exploratory calculations. Atomization energies were computed at the experimental geometries taken from the computational chemistry comparison and benchmark da-

TABLE I. Basis set dependence of the correlation energy of NH_3 using the PBE functional in the FDT-DFT scheme. The first three columns refer to the total molecular correlation energy, while the last three refer to the correlation contribution to the binding energy. "Raw" refers to the unextrapolated result, and subsequent columns give various extrapolations based on the raw results. Energies are in kcal/mol. The experimental result corresponds to a total correlation energy of −215 kcal/mol and a relative correlation energy of −97 kcal/mol (Ref. 48).

	Total correlation			Relative correlation		
cc-pVXZ	Raw	$(2X+1)^{-1}$	$(2X+1)^{-2}$	Raw	$(2X+1)^{-1}$	$(2X+1)^{-2}$
$X=3$	−148.6	⋯	⋯	−87.3	⋯	⋯
$X=4$	−138.1	−101.3	−122.0	−90.6	−102.0	−95.6
$X=5$	−122.7	−53.2	−91.4	−91.4	−95.3	−93.1
$X=6$	−106.7	−19.0	−66.5	−91.9	−94.4	−93.0

tabase (CCCBDB).[48] All open-shell systems were treated with a spin-unrestricted reference state allowing for full symmetry breaking and all correlation energies were determined within the frozen-core approximation.

V. RESULTS

A. Basis set convergence

We employed Dunning's correlation-consistent polarized valence X-tuple zeta (cc-pVXZ) basis sets $[X=3(\mathrm{T}),4(\mathrm{Q}),5,6]$[49] to facilitate extrapolation to the infinite basis set limit.[50,51] In all these basis sets, the exchange contribution is always converged to within a few tenths of a kcal/mol, and hence the challenge lies in extrapolating the correlation part. Table I illustrates the typical situation, from which several conclusions can be drawn. First, it is obvious that the total correlation energies obtained are much too positive. ALDA calculations for the uniform gas at metallic densities lead to a very similar picture, with an underestimation of the correlation energy by approximately the same amount that the RPA overestimates it.[21,24] Second, because of the unphysical cusp behavior, the convergence of $E_c(X)$ is *extremely* slow, and the basis sets we are using are still *very* far from convergence. However, since both these failures ultimately derive from a very short-ranged effect, one hopes that the resulting errors will largely cancel when energy differences are considered. This turns out to be the case, as illustrated in the last few columns of Table I.

Even for differential correlation, the basis set convergence of the energy is still extremely slow, as would be expected from the predicted $1/(2l_{\max}+1)$ asymptotic error of the partial-wave expansion of the correlation energy. Unfortunately, the theoretical large $l_{\max}$ limiting behavior is not quantitatively observed in our calculations. As shown in Table I, extrapolation using the simple form

$$E_c(X) = E_c(\infty) + \frac{A}{2X+1} \tag{37}$$

does not produce a rapidly convergent prediction of the complete basis result. This failure is primarily attributable to the fact that the cc-pVXZ sets (extended though they are) still do not contain high enough angular momentum components for the asymptotic partial-wave expansion to be valid. For example, for finite $l_{\max}$, the $(2l_{\max}+1)^{-1}$ term can be obscured by the $(2l_{\max}+1)^{-3}$ contribution that comes from the Coulombic interelectron cusp,[38] causing extrapolation based on the pure large $l_{\max}$ behavior to fail. Indeed, this effect is evident in the data presented in Table I. The $(2l_{\max}+1)^{-3}$ term, which contains RPA-like correlations and is primarily energy lowering, partially cancels the $(2l_{\max}+1)^{-1}$ contribution, which comes from f^{xc} and is typically positive. As a result the incremental correlation energies, $E_c(X)-E_c(X-1)$, are actually *larger* for cc-pV6Z than for cc-pV5Z due to smaller cancellation of terms in the larger basis.

In practice, we find that the form

$$E_c(X) = E_c(\infty) + \frac{A}{(2X+1)^2} \tag{38}$$

is a good compromise, taking into account the averaged effect of the $(2X+1)^{-1}$ and $(2X+1)^{-3}$ contributions in a stable way. The results using this extrapolation scheme are shown in the last column of the figure and the resulting predictions are more satisfactory (especially for the relative energetics). However, it should be stressed that the extrapolated results presented here should not be considered complete basis results; rather they correspond to "the best one can do" in the present circumstances. Unlike *ab initio* approaches, where the extrapolation is only needed to get the last few kcal/mol of the total energy, here the data clearly indicate that we are trying to predict a complete basis result that is many tens of kcal/mol from the best finite basis calculation we can perform. Further, based on the analysis of the last section, we cannot even rule out the possibility that the basis set limit of the total correlation energy is not well defined for semilocal functionals. Based on the variance in atomization energies predicted by different extrapolation schemes, we estimate that there is a residual uncertainty of at least 2-3 kcal/mol in the energies presented here.

B. Atomization energies

The FDT-DFT results for the atomization energies of 18 small molecules using several standard functionals are presented in Table II. The local-density approximation gives binding energies that are somewhat worse than RPA ($f^{\mathrm{xc}}=0$) overall. Further, including gradient corrections, as is done in Perdew–Burke–Ernzerhof (PBE)[52] and Becke–Perdew 1986 (BP86) GGAs,[53,54] has little effect on the results. These pure functionals tend to overbind by approximately the same amount as that by which RPA and time-dependent Hartree–Fock method (TDHF) underbind. Thus, we conclude that a completely local model of the XC kernel is not adequate. Meanwhile, including exact exchange in the calculation, as in Perdew–Burke–Ernzerhof 2000 (PBE0)[55] and in Becke's three-parameter hybrid (B3LYP),[56] tends to reduce the binding energy substantially, resulting in a significantly improved agreement with experiment. The PBE0 predictions are particularly good, with a mean absolute error (MAE) of 3.3 kcal/mol over the whole set. Thus, even the relatively simple nonlocality that is present in hybrid functionals allows for a more accurate description of FDT-DFT correlation energies. This may be compared to results for the

TABLE II. FDT-DFT atomization energies (in kcal/mol) using various approximate functionals. Molecules which have an error greater than twice the standard deviation for the given method are indicated in bold. RPA energies are computed using PBE orbitals. Experimental values (including zero-point vibrational corrections) are from Ref. 52.

Molecule	RPA	TDHF	LSDA	PBE	BP86	B3LYP	PBE0	Expt.
C_2H_2[a]	**381**	394	421	427	423	396	409	405
C_2H_2[b]	**538**	555	578	581	573	**549**	568	563
CH_4[a]	405	416	426	426	419	408	422	419
Cl_2[b]	50	57	[c]	74	74	56	64	58
CO[b]	244	249	287	**287**	**286**	258	264	259
F_2[b]	31	22	**74**	63	**76**	42	43	39
H_2[b]	109	108	110	110	107	110	111	109
H_2O[b]	224	226	249	245	241	230	235	232
HCN[b]	299	298	322	325	321	304	315	312
HF[b]	133	138	157	152	157	143	144	141
LiF[a]	130	136	158	159	**165**	**152**	**148**	139
LiH[a]	57	58	61	63	63	66	62	58
N_2[b]	223	210	229	230	228	220	228	229
NH_3[b]	290	289	296	293	286	**285**	297	297
NO[a]	148	132	[c]	163	163	147	154	153
O_2[a]	113	**97**	**155**	**151**	**150**	119	125	121
OH[b]	104	103	117	114	112	106	109	107
P_2[a]	116	105	118	118	116	112	118	117
MAE	9.1	9.2	13.5	12.3	12.9	6.0	3.3	⋯

[a]4/5 extrapolation.
[b]5/6 extrapolation.
[c]KS-LDA reference is unstable for Cl atom and NO molecule.

RPA+ functional proposed by Yan, Perdew, and Kurth,[57] which uses a conventional GGA for short-range correlation effects beyond RPA. As RPA, RPA+ has a well-behaved pair density, but it does not improve consistently upon atomization energies.[15]

These results should be compared with the results of conventional DFT using these functionals in a large cc-pV5Z basis, in which case one finds MAEs of 31.4 kcal/mol (local spin-density approximation, LSDA), 7.9 kcal/mol (PBE), 7.3 kcal/mol (BP86), 1.6 kcal/mol (B3LYP), and 3.1 kcal/mol (PBE0). Thus, the atomization energies predicted by FDT-DFT using standard functionals are typically somewhat worse than the conventional approach. This is not entirely surprising, as we have made no effort to calibrate the functionals to the new methodology. All the functionals considered here contain parameters that are selected either empirically based on experimental energetics or nonempirically using the known properties of the XC energy. In both cases, the functionals are in some sense optimal for describing the energetics in the conventional DFT framework. The fact that we want to use these functionals in conjunction with the FDT may imply an entirely different set of empirical and nonempirical constraints. For example, while one particular parametrization may lead to an accurate description of the energy of a nearly-uniform system, this is not necessarily the best set of parameters for describing the *response* of the system.

Similar considerations have motivated the "energy-optimized" parametrization of local, static exchange-correlation kernels by Dobson and Wang.[24] We have not been able to test these kernels in atomization energy calculations because no spin-resolved version was available to us. However, all of these kernels are local, and thus *any* parametrization will retain the unphysical pair density and slow basis set convergence. Any effort toward designing FDT-DFT functionals should foremost be directed at fixing these problems.

C. Dispersion

In some sense, comparing FDT-DFT with conventional DFT for electron pair bond energies is not very useful. It is well known that standard DFT already describes bond energies very well, and our primary focus is on improving DFT in situations where it works poorly, such as bond breaking,[58] transition state energetics,[59] and nonbonded interactions.[60] In the specific case of long-range dispersion forces, it has long been realized that conventional DFT (at least with local functionals) does not contain the proper physics to describe the binding of van der Waals clusters.[60,61] However, several authors have noted that dispersion interactions, in the form of C_6 coefficients, can be obtained from TDDFT response functions.[62–64] These dispersion coefficients are actually quite accurate, with typical errors in the order of 3% when standard functionals are used to compute the response.[65] Along these lines, TDDFT has successfully been used to compute intermolecular forces in the framework of symmetry-adapted perturbation theory.[66] The dissatisfying aspect of these approaches is that dispersion is included after the fact rather than as a limiting case of a more accurate energy functional. With FDT-DFT, though, the *entire* corre-

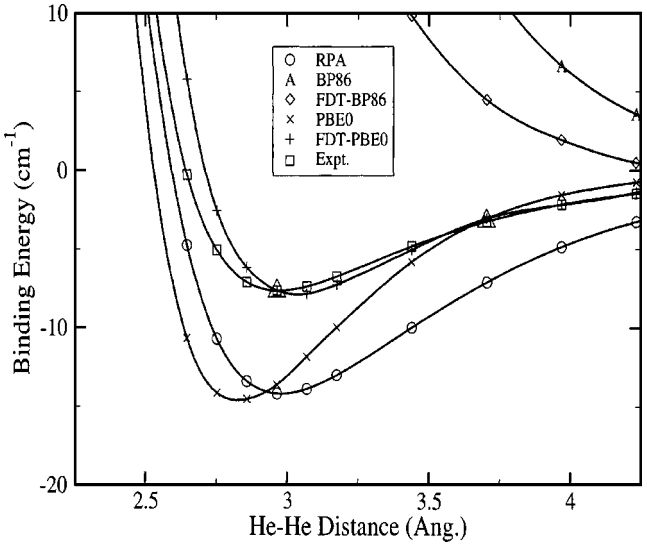

FIG. 1. Van der Waals interaction in the helium dimer. Energies are computed using two functionals, BP86 and PBE0, using either the fluctuation-dissipation theorem (FDT-BP86 and FDT-PBE0) or conventional means. The RPA results computed using BP86 orbitals are presented for comparison. Experimental results are from Ref. 70. Triangles denote accurate *ab initio* results from Ref. 71.

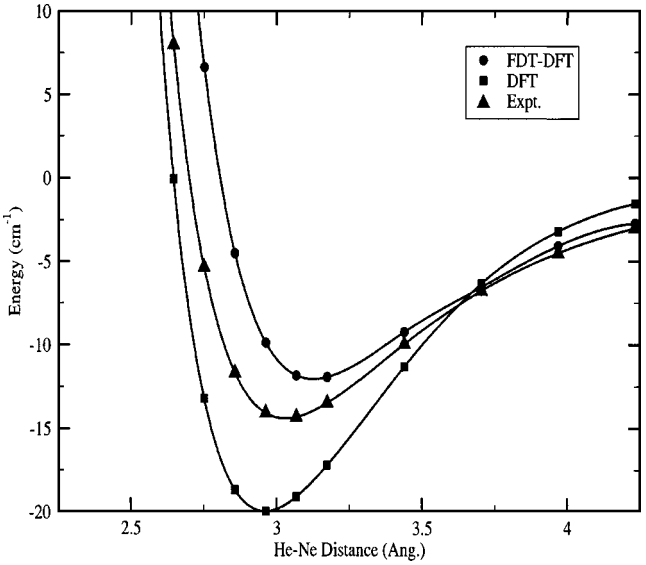

FIG. 2. Van der Waals interaction in HeNe. Energies are computed using the PBE0 functional using either the fluctuation-dissipation theorem (FDT-DFT) or conventional means (DFT). Experimental results are from Ref. 72.

lation energy is computed using the TDDFT response function; it is therefore the natural framework for treating dispersion interactions in DFT. In fact, the "seamless" van-der-Waals density functionals recently proposed by Dobson and Wang and[24,67] and by Langreth and co-workers[68,69] start out by approximating the FDT-DFT expression for the correlation energy [Eq. (4)].

To illustrate this point, Figs. 1 and 2 present FDT-DFT predictions of the dissociation curves for He_2 and HeNe, respectively. The calculations were performed in the augmented cc-pV6Z basis, with a large radial grid to ensure accurate integration of the XC energy. We have *not* corrected our results for basis set superposition error (BSSE). Because of the slow convergence of the total correlation energy with $l_{\max}$, the counterpoise correction is unphysically large for FDT-DFT and is not expected to be an accurate predictor of the BSSE. Nevertheless, we conclude that our calculations are fairly well-converged with respect to basis set, as the FDT-DFT binding energies change by ca. 1% in going from aug-cc-pV5Z to aug-cc-pV6Z. The more rapid convergence of the present calculations as compared to that of the calculations in the previous section is to be expected, since dispersion is a long-range correlation phenomenon and hence unlikely to be strongly affected by the short-range divergence of the pair density.

Perhaps the most important point that can be gleaned from the figures is that dispersion energies in FDT-DFT depend strongly on the choice of functional. Pure density functionals give such a poor description of f^{xc} that they do not predict reasonable binding curves in simple rare gas dimers. This is illustrated by the BP86 curves in Fig. 1. Although the FDT-DFT result is an improvement over conventional DFT, even the RPA ($f^{\mathrm{xc}}=0$) gives a much better description of dispersion than FDT-DFT using this functional. This is not entirely surprising; the atomization energies obtained above clearly demonstrate the poor quality of pure density functionals in the FDT-DFT scheme. Further, it has previously been shown that the dispersion energies predicted by hybrid functionals are a vast improvement over pure functionals.[65] In fact, second-order perturbation theory based on an LDA reference shows a very similar repulsive curve.[73] Note that one can prove that, for large enough distances, pure functionals do show the expected $-1/R^6$ energy dependence.[35] Our results simply indicate that, for pure functionals, the correct energy term is swamped at moderate distances by unphysical repulsive terms in f^{xc}.

However, for a hybrid functional (in this case, PBE0) we see that the FDT-DFT results describe dispersion effects in He_2 essentially quantitatively. The inner wall is somewhat too steep, but the depth of the well and the long-range tail are described very well. Furthermore FDT-DFT makes a qualitatively different prediction than conventional DFT, using the same functional. The conventional PBE0 calculation predicts a binding energy that is nearly 100% too large and does not exhibit the expected $1/R^6$ decay at large separations. We therefore conclude that hybrid functionals are absolutely crucial for the accurate description of dispersion effects. For HeNe, we have therefore focused our attention only on the hybrid functionals. The results are somewhat less accurate, but lead to similar conclusions. The FDT-DFT binding energy is underestimated and the van der Waals radius is significantly too large. However, the long-range behavior of the potential is again very accurately described by the FDT-DFT approach, which again points to the proper treatment of long-range dispersion effects in FDT-DFT.

VI. CONCLUSIONS AND OUTLOOK

In this article, the FDT-DFT formalism beyond the RPA has been implemented and applied to molecular systems. We have tested several approximate XC kernels within the AA. Kernels derived from semilocal functionals are too short-

ranged and lead to an unphysical divergence of the PDF at small interparticle distances. Although this is a very serious problem from both a fundamental and computational viewpoint, it has received little attention so far. The unphysical behavior of the PDF leads to a very slow basis set convergence of the correlation energy, which severely limits the usefulness of semilocal kernels in FDT-DFT. By using basis sets with up to i functions, we have nevertheless been able to estimate trends in atomization energies for a number of small molecules. Although FDT-DFT contains 100% of exact exchange by definition, atomization energies are predicted with an accuracy that is comparable to (if somewhat worse than) the results one is used to in standard DFT. GGA kernels tend to overbind approximately by the same amount that by which RPA underbinds. We were further able to verify that FDT-DFT, using standard functionals, is capable of accurately describing long-range dispersion effects on the same footing with molecular binding energies.

Despite the somewhat disappointing failure of local kernels, FDT-DFT has many appealing aspects and may deserve continued effort. It is not clear to what extent the AA affects the accuracy of FDT-DFT; the fact that accurate correlation energies can be obtained within the AA, at least in the high-density limit, suggests it as a reasonable (and efficient) starting point. Similar conclusions have been drawn by Lein *et al.* for the uniform gas.[21] Thus, it would seem that further work should focus on the construction of kernels that satisfy two key properties: (i) nonlocality and (ii) stability. The most natural and promising nonlocal functionals would seem to be those that incorporate some treatment of exact exchange. This would (1) remove the unphysical divergence of the pair distribution function (and thus facilitate basis set convergence), (2) allow one to cancel the spurious self-correlation present in a semilocal FDT-DFT calculation, and (3) reproduce the exact doubles contribution to the second-order correlation energy [Görling–Levy (GL2), Ref. 74]. Unfortunately, the full exact exchange kernel required for exact exchange FDT-DFT is frequency dependent and difficult to implement.[75] There are, of course, simplified nonlocal exchange kernels, for example, the Petersilka–Gossman–Gross (PGG) kernel.[13,40] However, in this case, one loses stability; there is no simple nonlocal exchange kernel available that is derivable from an XC potential. We have implemented one such potential and verified that while self-correlation can be effectively removed, in approximately 10% of the cases the mismatch between f^{xc} and χ_0 leads to an imaginary correlation energy. Thus, one clear future direction is the development of a simple nonlocal potential that approximately accounts for exchange and correlation effects. Nonlocal kernels can be easily incorporated into our computational framework, as long as the integral evaluation time does not exceed the rate-determining $O(N^6)$ generation of the response.

ACKNOWLEDGMENTS

T.V. would like to gratefully acknowledge start-up funds from MIT. F.F. was supported by the Center for Functional Nanostructures (CFN) of the Deutsche Forschungsgemeinschaft (DFG) through Project No. C2.1.

[1] E. Runge and E. K. U. Gross, Phys. Rev. Lett. **52**, 997 (1984).
[2] E. K. U. Gross and W. Kohn, Adv. Quantum Chem. **21**, 255 (1990).
[3] M. A. L. Marques and E. K. U. Gross, Annu. Rev. Phys. Chem. **55**, 427 (2004).
[4] F. Furche and D. Rappoport, in *Computational Photochemistry*, edited by M. Olivucci (Elsevier, Amsterdam, to be published).
[5] F. Furche and K. Burke, *Annual Reports in Computational Chemistry*, Vol. 1 (Elsevier, New York, 2005).
[6] A. L. Fetter and J. D. Walecka, *Quantum Theory of Many-Particle Systems* (McGraw-Hill, New York, 1971).
[7] M. Levy, Proc. Natl. Acad. Sci. U.S.A. **76**, 6062 (1979).
[8] W. Kohn and L. J. Sham, Phys. Rev. **140**, A1133 (1965).
[9] D. C. Langreth and J. P. Perdew, Solid State Commun. **17**, 1425 (1975).
[10] D. C. Langreth and J. P. Perdew, Phys. Rev. B **15**, 2884 (1977).
[11] F. Furche, J. Chem. Phys. **114**, 5982 (2001).
[12] E. K. U. Gross and W. Kohn, Phys. Rev. Lett. **55**, 2850 (1985).
[13] M. Petersilka, U. J. Gossmann, and E. K. U. Gross, Phys. Rev. Lett. **76**, 1212 (1996).
[14] For hybrid functionals, one obtains a similar Dyson-type equation that relates the density-*matrix* response of the interacting and noninteracting systems rather than simply the density response.
[15] F. Furche, Phys. Rev. B **64**, 195120 (2001).
[16] D. Bohm and D. Pines, Phys. Rev. **82**, 625 (1951).
[17] K. Raghavachari, G. W. Trucks, J. A. Pople, and M. Head-Gordon, Chem. Phys. Lett. **157**, 479 (1989).
[18] V. Barone, Chem. Phys. Lett. **233**, 129 (1995).
[19] F. A. Cotton and X. J. Feng, J. Am. Chem. Soc. **119**, 7514 (1997).
[20] J. M. Pitarke and J. P. Perdew, Phys. Rev. B **67**, 045101 (2003).
[21] M. Lein, E. K. U. Gross, and J. P. Perdew, Phys. Rev. B **61**, 13431 (2000).
[22] R. Asgari, M. Polini, B. Davoudi, and M. P. Tosi, Phys. Rev. B **68**, 155112 (2003).
[23] J. M. Pitarke and A. G. Eguiluz, Phys. Rev. B **57**, 6329 (1998).
[24] J. F. Dobson and J. Wang, Phys. Rev. B **62**, 10038 (2000).
[25] J. F. Dobson, J. Wang, and T. Gould, Phys. Rev. B **66**, 081108(R) (2002).
[26] M. Fuchs and X. Gonze, Phys. Rev. B **65**, 235109 (2002).
[27] C. F. Richardson and N. W. Ashcroft, Phys. Rev. B **50**, 8170 (1994).
[28] Note that, for hybrid functionals, the orbitals are not technically Kohn–Sham orbitals since they are derived from a nonlocal potential.
[29] J. F. Dobson, M. J. Bunner, and E. K. U. Gross, Phys. Rev. Lett. **79**, 1905 (1997).
[30] M. Levy and J. P. Perdew, in *Single-Particle Density in Physics and Chemistry*, edited by N. H. March and B. M. Deb (Academic, London, 1987), pp. 54–55.
[31] P. Hessler, J. Park, and K. Burke, Phys. Rev. Lett. **82**, 378 (1999); **83**, 5184 (1999).
[32] K. S. Singwi, M. P. Tosi, R. H. Land, and A. Sjölander, Phys. Rev. **176**, 589 (1968).
[33] R. Bauernschmitt and R. Ahlrichs, J. Chem. Phys. **104**, 9047 (1996).
[34] R. van Leeuwen and E. J. Baerends, Phys. Rev. A **49**, 2421 (1994).
[35] Y. M. Niquet, M. Fuchs, and X. Gonze, Phys. Rev. A **68**, 032507 (2003).
[36] S. Hellal, J.-G. Gasser, and A. Issolah, Phys. Rev. B **68**, 094204 (2003).
[37] P. Gori-Giorgi and J. P. Perdew, Phys. Rev. B **66**, 165118 (2002).
[38] T. Kato, Commun. Pure Appl. Math. **10**, 151 (1957).
[39] A. J. Thakkar and V. H. Smith, Chem. Phys. Lett. **42**, 476 (1976).
[40] E. K. U. Gross, J. F. Dobson, and M. Petersilka, Top. Curr. Chem. **181**, 81 (1996).
[41] J. C. Kimball, Phys. Rev. A **7**, 1648 (1973).
[42] D. A. Atkinson and H. D. Crater, Am. J. Phys. **43**, 301 (1975).
[43] W. Kutzelnigg and J. D. Morgan III, J. Chem. Phys. **96**, 4484 (1992).
[44] W. Kutzelnigg, Theor. Chim. Acta **68**, 445 (1985).
[45] R. Ahlrichs, M. Häser, H. Horn, and C. Kolmel, Chem. Phys. Lett. **162**, 165 (1989).
[46] http://www.turbomole.com
[47] O. Treutler and R. Ahlrichs, J. Chem. Phys. **102**, 346 (1995).
[48] http://srdata.nist.gov/cccbdb/
[49] T. H. Dunning, Jr., J. Chem. Phys. **90**, 1007 (1989).
[50] T. Helgaker, W. Klopper, H. Koch, and J. Noga, J. Chem. Phys. **106**, 9639 (1997).
[51] A. Halkier, T. Helgaker, P. Jorgensen, W. Klopper, H. Koch, J. Olsen, and A. Wilson, Chem. Phys. Lett. **286**, 243 (1998).
[52] J. P. Perdew, K. Burke, and M. Ernzerhof, Phys. Rev. Lett. **77**, 3865 (1996).
[53] A. D. Becke, Phys. Rev. A **38**, 3098 (1988).
[54] J. P. Perdew, Phys. Rev. B **33**, 8822 (1986).

[55]J. P. Perdew, M. Ernzerhof, and K. Burke, J. Chem. Phys. **105**, 9982 (1996).
[56]A. D. Becke, J. Chem. Phys. **98**, 5648 (1993).
[57]Z. Yan, J. P. Perdew, and S. Kurth, Phys. Rev. B **61**, 16430 (2000).
[58]V. Polo, E. Kraka, and D. Cremer, Theor. Chem. Acc. **107**, 291 (2002).
[59]J. L. Durant, Chem. Phys. Lett. **256**, 595 (1996).
[60]S. Tsuzuki and H.-P. Lüthi, J. Chem. Phys. **114**, 3949 (2001).
[61]Y. K. Zhang, W. Pan, and W. Yang, J. Chem. Phys. **107**, 7921 (1997).
[62]S. J. A. van Gisbergen, J. G. Snijders, and E. J. Baerends, J. Chem. Phys. **103**, 9347 (1995).
[63]S. J. A. van Gisbergen, V. P. Osinga, O. V. Gritsenko, R. van Leeuwen, J. G. Snijders, and E. J. Baerends, J. Chem. Phys. **105**, 3142 (1996).
[64]W. Kohn, Y. Meir, and D. E. Makarov, Phys. Rev. Lett. **80**, 4153 (1998).
[65]A. J. Misquitta, B. Jeziorski, and K. Szalewicz, Phys. Rev. Lett. **91**, 033201 (2003).
[66]A. Hëselmann and G. Jansen, Chem. Phys. Lett. **367**, 778 (2003).
[67]J. F. Dobson and J. Wang, Phys. Rev. Lett. **82**, 2123 (1999).
[68]D. C. Langreth, M. Dion, H. Rydberg, E. Schröder, P. Hyldgaard, and B. I. Lundqvist, Int. J. Quantum Chem. **101**, 599 (2005).
[69]M. Dion, H. Rydberg, E. Schröder, D. C. Langreth, and B. I. Lundqvist, Phys. Rev. Lett. **92**, 246401 (2004).
[70]J. F. Ogilvie and F. Y. H. Wang, J. Mol. Struct. **273**, 277 (1992).
[71]W. Cencek, M. Jeziorska, R. Bukowski, M. Jaszunski, B. Jeziorski, and K. Szalewicz, J. Phys. Chem. A **108**, 3211 (2004).
[72]J. F. Ogilvie and F. Y. H. Wang, J. Mol. Struct. **291**, 313 (1993).
[73]E. Engel and A. F. Bonetti, Int. J. Mod. Phys. B **15**, 1703 (2001).
[74]A. Görling and M. Levy, Phys. Rev. B **47**, 13105 (1993).
[75]F. Della Salla and A. Görling, Int. J. Quantum Chem. **91**, 131 (2003).